FORUM GEOGRAFIC

Forum geografic. Studii şi cercetări de geografie şi protecţia mediului
*Volume **XV**, Issue **1** (**June** 2016), pp. **45-53***
*http://dx.doi.org/**10.5775/fg.2016.137.i***

Evaluation of land use/land cover classification accuracy using multi-resolution remote sensing images

Varun Narayan MISHRA[1*], Praveen Kumar RAI[2], Pradeep KUMAR[1], Rajendra PRASAD[1*]

[1] Department of Physics, Indian Institute of Technology (BHU), Varanasi, India
[2] Department of Geography, Banaras Hindu University, Varanasi, India
* *Corresponding author*, rprasad.app@itbhu.ac.in

Received on <18-04-2016>, reviewed on <15-05-2016>, accepted on <30-05-2016>

Abstract

Timely and accurate land use/land cover (LULC) information is requisite for sustainable planning and management of natural resources. Remote sensing images are major information sources and they are widely used for mapping and monitoring various land features. Images from various sensors, with different spatial resolutions, are available; however, the selection of appropriate spatial resolution is an essential task to extract desired information from images. This paper presents the conclusions of the work related to LULC classification based on multi-resolution remote sensing images. Optical data collected by three different sensors (LISS IV with 5.8 m and Landsat 8-OLI with 30 m and AWiFS with 56 m spatial resolutions respectively) in 2013 are examined against the potential to correctly classify specific LULC classes. The classifications of images are performed using Maximum Likelihood Classifier (MLC). The results indicate that the overall accuracy and kappa coefficient of LISS IV with 5.8 m are higher than that of Landsat 8-OLI with 30 m and AWiFS with 56 m images. Understanding the role of spatial resolution in LULC classification accuracy will enable the appropriate interpretation of any classified images.

Keywords: *remote sensing, spatial resolution, accuracy, separability, analysis*

Rezumat. Evaluarea acurateţii clasificării modului de utilizare/acoperire a terenurilor folosind imagini de teledecţie multi-rezoluţie

Informaţii precise şi în timp util privind utilizarea/acoperirea terenului (LULC) sunt necesare pentru planificarea și gestionarea durabilă a resurselor naturale. Imaginile de teledetecţie sunt surse majore de informare și sunt utilizate pe scară largă pentru cartografierea și monitorizarea diferitelor caracteristici ale terenului. Imagini de la diverși senzori, cu diferite rezoluții spațiale, sunt disponibile; cu toate acestea, selectarea rezoluției spațiale corespunzătoare este o sarcină esențială pentru a extrage informațiile dorite din imagini. Această lucrare prezintă concluziile referitoare la clasificarea LULC bazată pe imagini de teledetecție multi-rezoluție. Datele optice colectate de trei senzori diferiți (LISS IV cu 5,8 m și Landsat 8-OLI cu 30 m și respectiv AWiFS cu 56 m rezoluție spațială), în 2013, sunt examinate în raport cu potențialul de a clasifica corect clasele specifice LULC. Clasificările imaginilor sunt realizate utilizând Clasificatorul de maximă probabilitate (MLC). Rezultatele indică faptul că precizia per total și coeficientul kappa al imaginilor LISS IV cu 5,8 m sunt mai mari decât cele ale Landsat 8-OLI cu 30 m și AWiFS cu 56 m. Înţelegerea rolului rezoluției spațiale în clasificarea precisă LULC va permite interpretarea adecvată a oricăror imagini clasificate.

Cuvinte-cheie: *teledecţie, rezoluţie spaţială, acurateţe, separabilitate, analiză*

Introduction

Earth observation data acquired from different sensors at various spatial resolutions have been used broadly in the studies of global environmental changes, management of natural resources and ecological systems. Timely and accurate LULC information is vital for several planning and management activities and also for understanding the functioning of Earth as a system (Salberg and Jenssen, 2012; Lambin et al., 2001).

During the last few decades, remote sensing technologies have made remarkable development and now a number of images from different sensors with high, medium and coarse spatial resolution are available (Clark et al., 2004). The selection of improper spatial resolution can lead to ambiguous interpretation and hence LULC classification using a single remote sensing image has some limitations such as low classification accuracy and adaptability. Therefore, with increasing number of different spatial resolution images, the selection of the appropriate one has become more complex (Chen et al., 2004). One of the basic characteristics of a remote sensing image is its spatial resolution, which extensively affects the accuracy of image classification. In the case of remotely sensed images, the classification accuracy is strongly affected by the influence of boundary pixels and the finer spatial resolution which increases the spectral-radiometric variation of LULC classes (Markham and Townshend, 1981). The linkage between classification accuracy and spatial resolution of the image strongly depends on the size and spatial patterns of LULC classes (Moody and Woodcock, 1994). The suitable spatial resolution is also a function of the type of desired information and the techniques used to extract information.

In an optical remote sensing system, the spatial resolution is defined as the smallest resolvable spatial unit on the ground recorded in an image (Woodcock and Strahler, 1987) and determines the level of observed spatial detail on the Earth's surface. The spatial resolution provides the patterns

and distributions of objects (Singh et al., 2002; Frank and Tweddale, 2006). The fundamental information contained in a remote sensing image is robustly dependent on spatial resolution and it extensively affects each stage of image classification. Image classification is a widely used way to get spatially distributed LULC information (Borak and Strahler, 1999). With the launch of Landsat satellites series, several image classification techniques have been developed (Lu and Weng, 2007). The maximum likelihood classifier (MLC) is parametric in nature, representing the most widely used classification technique (Jensen, 2005; Foody et al., 1992). It assumes normal Gaussian distribution of multivariate data with pixels allocated to the most probable output LULC categories (Richards and Jia, 2003). In several studies, MLC has been used effectively for classifying LULC and other categories (Chen et al., 2004; Mishra et al., 2014a; Kumar et al., 2016; Mishra and Rai, 2016).

Therefore, the effects of spatial resolution on LULC classification accuracy have received considerable attention due to the availability of a large variety of Earth observation data. This study employs multi-resolution remote sensing images to determine how varying spatial resolution affects the accuracy of LULC classification. The classification accuracy at each spatial resolution is reported and compared.

Study area

The study area is a part of Varanasi district, Uttar Pradesh, India. Geographically, it lies between 25° 12′ 01.08″ N to 25° 20′ 43.88″ N latitudes and 82° 54′ 30.32″ E to 83° 04′ 08.64″ E longitudes and spreads over an area of 26098 ha. It is one of the oldest living cities in the world, being located on the bank of Holy River Ganga. This area is very productive and wealthy in agriculture because of its location in the Indo-Gangetic plain. The location map of the study site is shown in Figure 1.

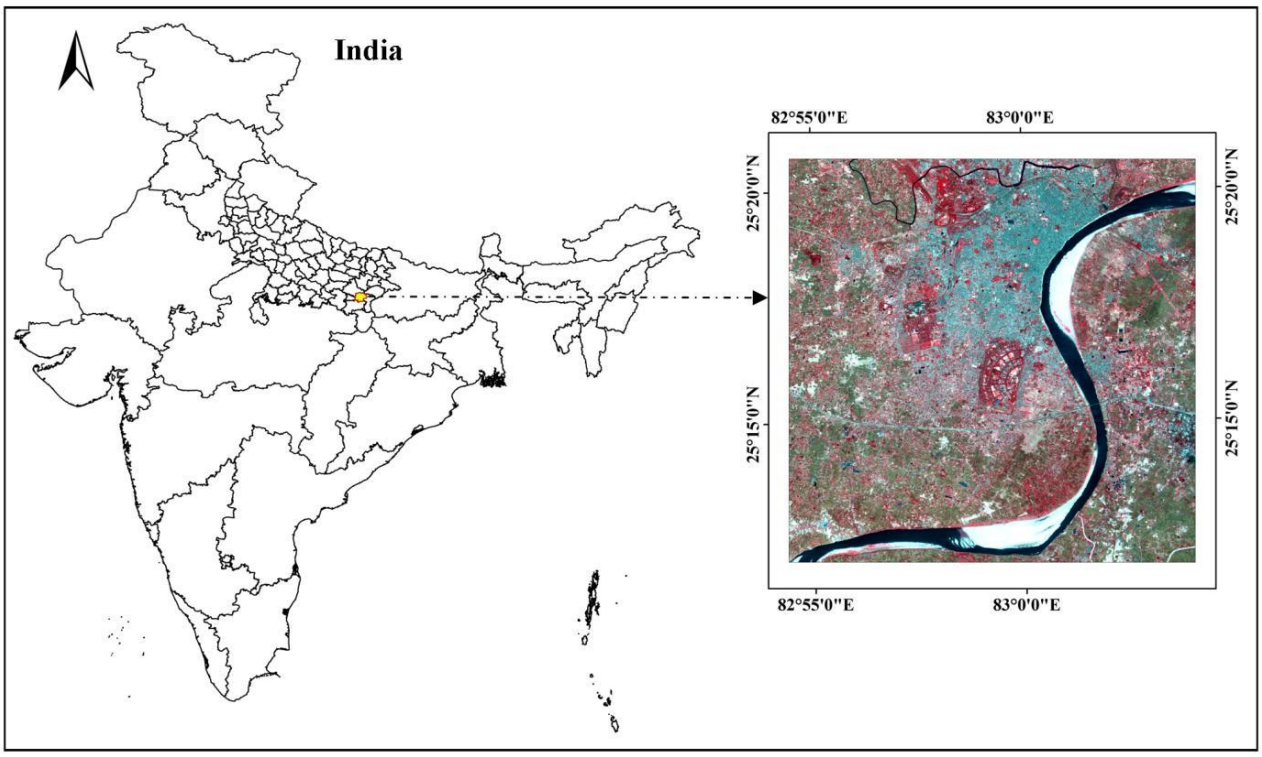

Fig. 1: Location of study area as viewed on IRS-LISS IV image

Materials and Methodology

Remote sensing images from three different sensors having a range of spatial resolutions were used in this study. To perform LULC classification, LISS IV with 5.8 m, Landsat 8-OLI with 30 m and AWiFS with 56 m spatial resolution images acquired on 6 April, 2013, 15 April, 2013 and 10 May, 2013 respectively are used. The ground truth information is also collected with the help of the Global Positioning System (GPS) and high resolution Google earth images. The characteristics of the datasets are presented in Table 1 and images are shown in Figures 2 (a), (b) and (c) respectively.

Table 1: Specifications of datasets used in this study

Satellite-Sensor	Bands	Spectral Resolution (μm)	Spatial Resolution (m)
Resourcesat-2 Linear Imaging Self Scanning (LISS IV)	B 2-Green	0.52-0.59	5.8
	B 3-Red	0.62-0.68	5.8
	B 4-NIR	0.77-0.86	5.8
Landsat-8 Operational Land Imager- Thermal Infrared Sensor (OLI-TIRS)	B 1-Coastal aerosol	0.43-0.45	30
	B 2-Blue	0.45-0.51	30
	B 3-Green	0.53-0.59	30
	B 4-Red	0.64-0.67	30
	B 5-NIR	0.85-0.88	30
	B 6-SWIR 1	1.57-1.65	30
	B 7-SWIR 2	2.11-2.29	30
	B 8-Panchromatic	0.50-0.68	15
	B 9-Cirrus	1.36-1.38	30
	B 10-TIRS 1	10.60-11.19	100
	B 11-TIRS 2	11.50-12.51	100
Resourcesat-1 Advanced Wide Field Sensor (AWiFS)	B 2- Green	0.52-0.59	56
	B 3- Red	0.62-0.68	56
	B 4- NIR	0.77-0.86	56
	B 5- SWIR	1.55-1.70	56

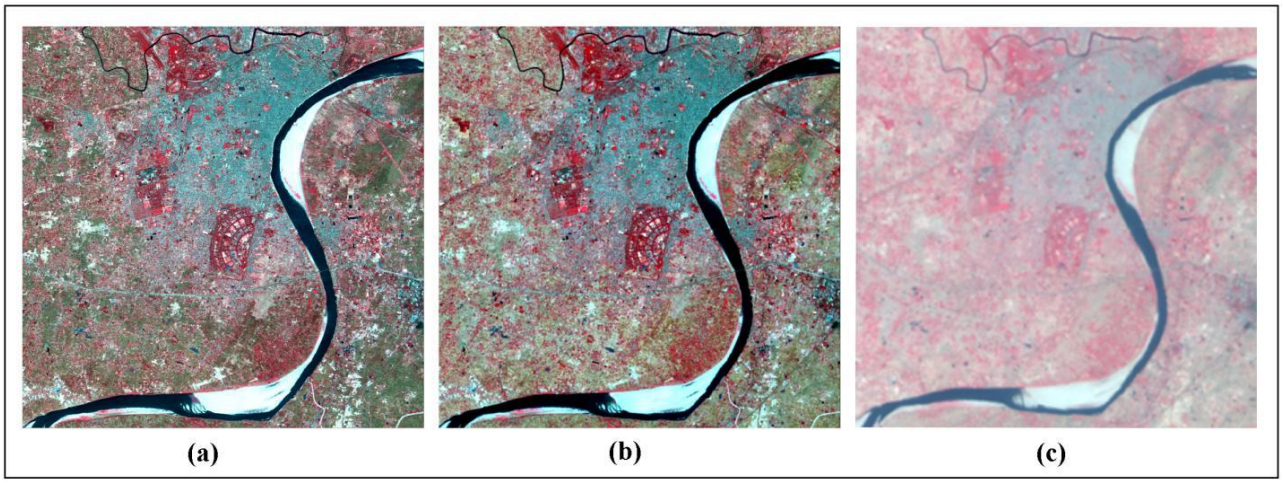

Fig. 2: Data sets in false colour composite (FCC) (a) LISS IV (b) Landsat 8-OLI (c) AWiFS

Image pre-processing

The processing and interpretation of multi-resolution images is performed by using ENVI (v5.1) image processing software. The images are first imported into ENVI and the layer stacking option available in basic tools is used to generate false colour composite (FCC) for all the images. The areas of interest (AOI) are extracted by subsetting the images. It is essential to perform geometric correction to obtain spatially distributed LULC maps. The image-to-image registration procedure is used to co-register all the datasets. During image transformation, the first-degree polynomial equation and nearest neighbour resampling method is used. The images are in the Universal Transverse Mercator (UTM) coordinate system (Zone 44, North), with World Geodetic System (WGS) 1984 datum. Only 9 bands of OLI sensor of Landsat-8 satellite are used in this study. The FCCs are preferred to create training samples for classification and analysis purpose.

Class separability analysis

A statistical measure named transformed divergence (TD) is used for inter-class separability analysis (Swain and Davis, 1978). It is a measure of statistical distance between two training samples (signatures). It may also be used to evaluate the separability between LULC classes prior to image classification. In several studies, the TD method is used to measure the separability between classes (Kumar et al., 2015; Mishra et al., 2014b). Its values vary from 0 to 2.0 and show how well the selected training samples are statistically separable from each other. Generally, a value greater than 1.9 means a good separability, while a value under 1.7 is regarded as poor separability between two classes. The equation below is used to conduct class separability analysis by using the TD method for all datasets:

$$TD_{ij} = 2000\left(1 - \exp\left(\frac{-D_{ij}}{8}\right)\right) \quad (1)$$

Here, D_{ij}= divergence between two signatures and it can be calculated by:

$$D_{ij} = \frac{1}{2}\,tr\left((C_i - C_j)(C_i^{-1} - C_j^{-1})\right) + \frac{1}{2}\,tr\left((C_i^{-1} - C_j^{-1})(\mu_i - \mu_j)(\mu_i - \mu_j)^T\right)$$

Where, i and j = the two signatures (classes) being compared, C_i = The covariance matrix of signature I, μ_i = The mean vector of signature I, tr = the trace function which calculates the sum of the elements on the main diagonal, T = the transpose of the matrix.

LULC classification

MLC is the most widely used supervised classification technique based on the likelihood of a pixel belonging to a specific class (Jensen, 2005). It is a parametric statistical approach that involves the normal distribution of class signatures. MLC is a pixel based technique relying on a multivariate probability density function of classes (Richards and Jia, 2003). This technique uses training samples or class signatures apprehended directly from the image to be classified. The probability of a pixel belonging to one of the classes is computed. Then, a particular class is assigned to the pixel with maximum probability. The equation used for MLC is given as:

$$D = \ln(a_c) - [0.5\ln(|Cov_c|)] - [0.5\,(X - M_c)]\,T\,(Cov_c^{-1})(X - M_c)] \quad (2)$$

Where, D = weighted distance, c = particular class, X = measurement vector of the candidate pixel, M_c= mean vector of the sample of class c, a_c = percent probability that any candidate pixel is a member of class c, Cov_c= covariance matrix of the pixels in the sample of class c, $|Cov_c|$ = determinant of Cov_c, Cov_c^{-1} = inverse of Cov_c, ln = natural logarithm function and T = transposition function.

Accuracy assessment of LULC classification results

The LULC classification results are evaluated to test the validity and dependability of the produced classified maps. The classification results are assessed by computing the overall accuracy (OA), user's accuracy (UA), producer's accuracy (PA), and Kappa coefficient (Kc) (Congalton and Green, 1999). It is not convenient to test each and every pixel of classified maps. So, a set of reference pixels or testing samples are collected with the help of field visits and Google earth images. The OA, PA, UA and Kc are computed using equations as (3), (4), (5) and (6) respectively as follows:

$$OA = \frac{1}{N}\sum_{i=1}^{r} n_{ii} \quad (3), \qquad PA = \frac{n_{ii}}{n_{icol}} \quad (4), \qquad UA = \frac{n_{ii}}{n_{irow}} \quad (5),$$

$$K_c = N\sum_{i=1}^{r} n_{ii} - \sum_{i=1}^{r} \frac{n_{icol}n_{irow}}{N^2} - \sum_{i=1}^{r} n_{icol}n_{irow} \quad (6)$$

Results and Disscusions

After collecting training samples of each LULC class, LISS IV, Landsat 8-OLI and AWiFS images are classified using supervised MLC. Each image is classified into seven major LULC classes like agricultural land, dense vegetation, sparse vegetation, fallow land, built up, water bodies and sand. The TD values are estimated for all LULC class pairs under the present study. The highest TD values are found for LISS IV image followed by Landsat 8-OLI and AWiFS images. The TD value greater than 1.9 indicates better separability between two LULC classes. The detailed information of separability analysis using TD method for all the datasets are given in Table 2.

The MLC based LULC maps of LISS IV, Landsat 8-OLI and AWiFS images are shown in Figures 3, 4 and 5. Accuracy assessment is the qualitative assessment of classification results based on remote sensing images. It is helpful in evaluating the classification techniques and determining the level of error that might be contributed by the image. The accuracy assessment results for MLC based classified maps of LISS IV with 5.8 m, Landsat 8-OLI with 30 m and AWiFS with 56 m spatial resolutions are shown in Table 3. The achieved OA for classified products from LISS IV, Landsat 8-OLI and AWiFS images are 83.28%, 77.93% and 74.61% respectively, with Kc of 0.805, 0.742 and 0.705 respectively. The area distribution of LULC classes for the datasets is presented in Table 4.

Table 2: Separability analysis between LULC classes using TD distance method

LULC Class pairs	TD values		
	LISS IV	Landsat 8-OLI	AWiFS
Agricultural land-Dense vegetation	1.99	1.98	1.99
Agricultural land-Open vegetation	1.94	1.75	1.60
Agricultural land-Fallow land	1.99	1.98	1.99
Agricultural land-Built up	1.99	1.99	1.99
Agricultural land-Water bodies	2.00	2.00	1.99
Agricultural land-Sand	2.00	2.00	2.00
Dense vegetation-Open vegetation	1.99	1.92	1.95
Dense vegetation-Fallow land	2.00	2.00	1.99
Dense vegetation-Built up	2.00	2.00	1.99
Dense vegetation-Water bodies	2.00	2.00	1.99
Dense vegetation-Sand	2.00	2.00	2.00
Open vegetation-Fallow land	1.99	1.99	1.89
Open vegetation-Built up	2.00	2.00	1.99
Open vegetation-Water bodies	2.00	2.00	1.99
Open vegetation-Sand	2.00	2.00	1.99
Fallow land-Built up	1.99	1.99	1.99
Fallow land-Water bodies	2.00	2.00	1.99
Fallow land-Sand	1.99	2.00	1.94
Built up-Water bodies	2.00	2.00	1.97
Built up-Sand	2.00	2.00	1.99
Water bodies-Sand	2.00	2.00	2.00

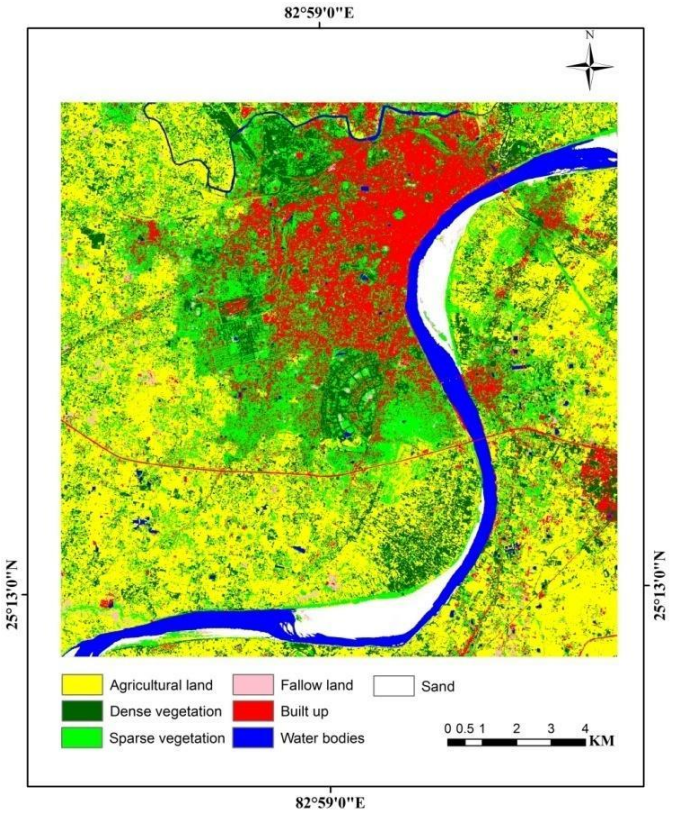

Fig. 3: MLC based LULC map of LISS IV image

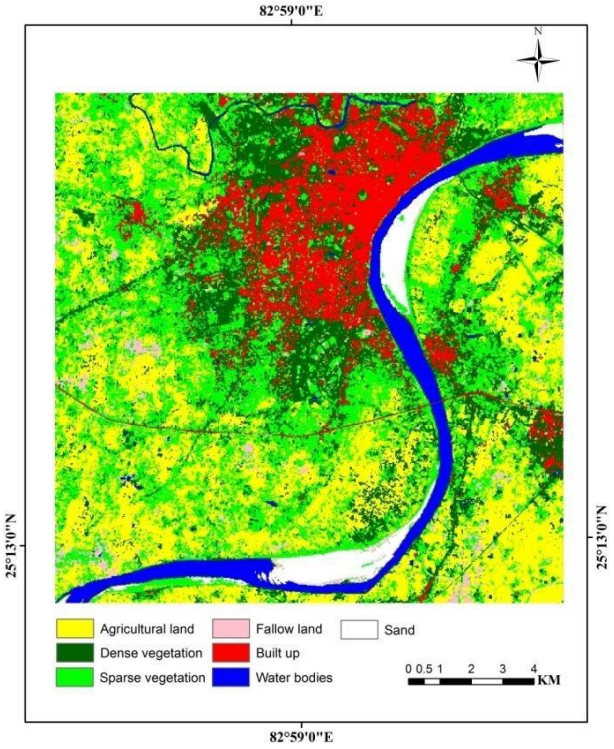

Fig.4: MLC based LULC map of Landsat 8-OLI image

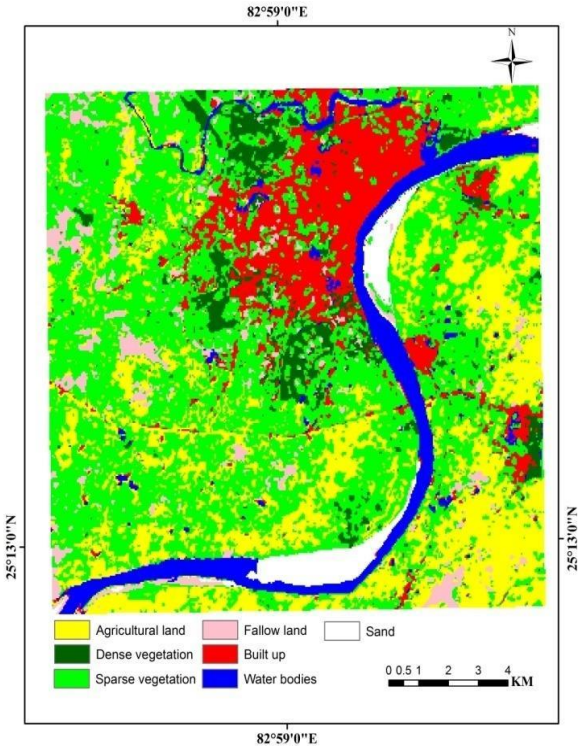

Fig. 5: MLC based LULC map of AWiFS image

Table 3: Accuracy assessment of LULC classification results

LULC classes	LISS IV		Landsat 8-OLI		AWiFS	
	PA (%)	UA (%)	PA (%)	UA (%)	PA (%)	UA (%)
Agricultural land	80.86	79.34	75.76	74.69	72.78	72.56
Dense vegetation	82.80	85.98	78.78	81.40	77.58	79.64
Sparse vegetation	83.02	77.83	78.10	74.10	75.41	70.31
Fallow land	81.24	76.67	73.46	66.19	66.16	63.02
Built up	84.96	86.20	79.36	79.49	75.76	75.13
Water bodies	84.88	91.06	80.40	88.61	78.31	84.66
Sand	84.58	85.13	78.25	79.54	74.14	75.50
OA (%)	83.28		77.93		74.61	
Kc	0.805		0.742		0.705	

Table 4: Area distribution of LULC using LISS IV, Landsat 8-OLI and AWiFS images

LULC classes	LISS IV		Landsat 8-OLI		AWiFS	
	Area (ha)	Area (%)	Area (ha)	Area (%)	Area (ha)	Area (%)
Agricultural land	10390	39.81	7947	30.45	6257	23.98
Dense vegetation	4032	15.45	5035	19.29	1384	5.30
Sparse vegetation	5237	20.07	7803	29.90	11490	44.03
Fallow land	412	1.58	605	2.32	1179	4.52
Built up	3819	14.63	2857	10.95	3235	12.40
Water bodies	1312	5.03	1222	4.68	1822	6.98
Sand	896	3.43	629	2.41	731	2.80
Total Area	26098	100.00	26098	100.00	26098	100.00

The PA is a calculation of omission error while UA is a measure of commission error of an individual LULC class. The classified result derived by LISS IV image indicates that PA varied from 80.86% for agricultural land to 84.96% for built up, while, UA varied from 76.67% for fallow land to 91.06% for water bodies. The classified result derived by Landsat 8-OLI image indicates that PA varied from

73.46% for fallow land to 80.40 % for water bodies, while, UA ranged from 66.19% for fallow land to 88.61% for water bodies. The classified result derived by using AWiFS image indicates that PA varied from 66.16% for fallow land to 78.31% for water bodies, while, UA varied from 63.02% for fallow land to 84.66% for water bodies.

Furthermore, the effects of spatial resolution are also observed on the interpretation and degree of information for classified images. Figure 6 shows the degree of interpretation of different LULC classes in various spatial resolutions, by visual comparison of LULC thematic maps at two different sites. The lower UA values of fallow land are found for Landsat 8-OLI and AWiFS images, as compared to that found for LISS IV image, which is higher. It reveals that the interpretation and identification of fallow land is easier by using the high spatial resolution image of LISS IV than the moderate and coarse spatial resolution images of Lamdsat8-OLI and AWiFS.

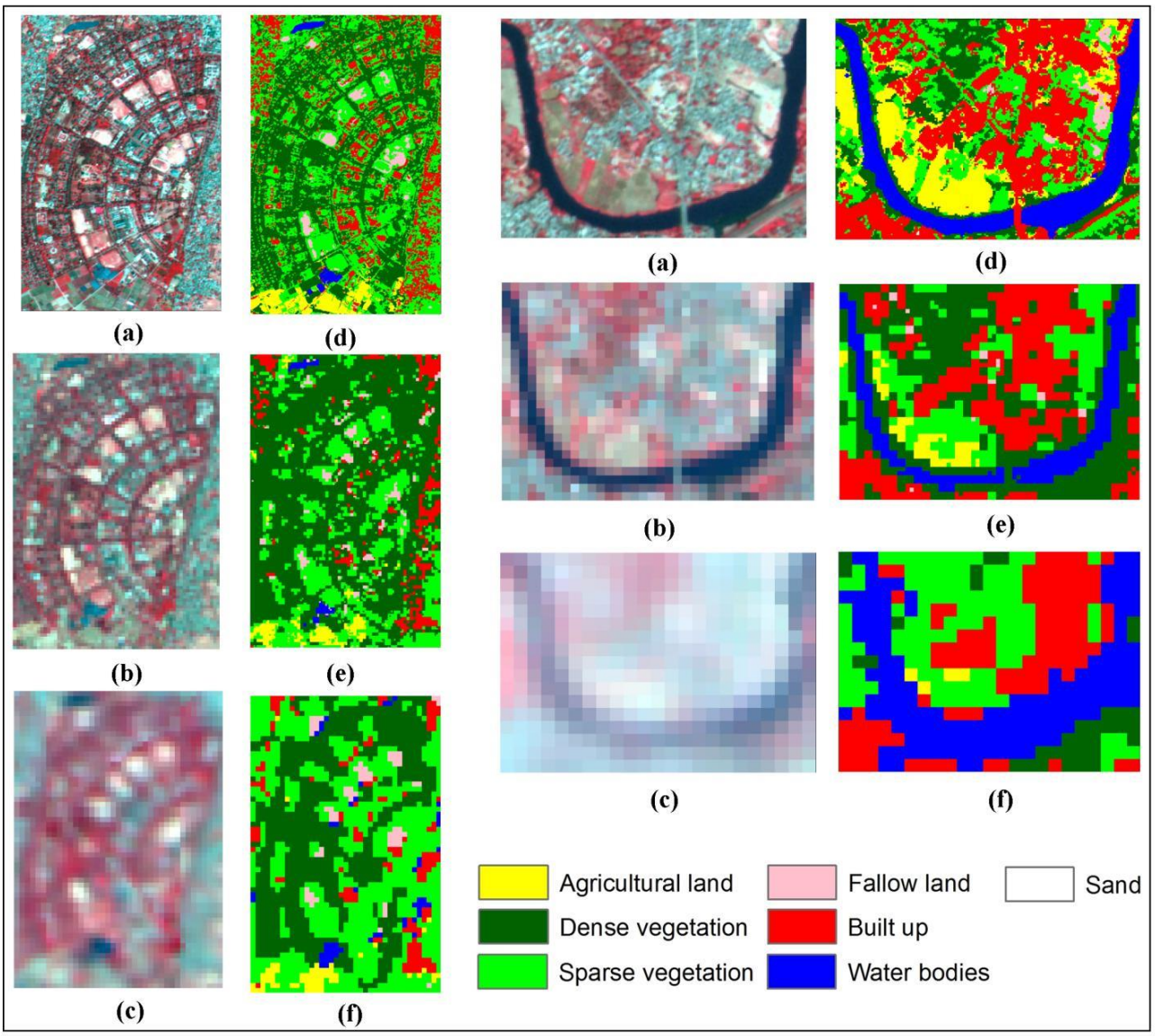

Fig. 6: Visual comparison at two selected sites: (a) LISS IV Image; (b) Landsat 8-OLI image; (c) AWiFS image and (d) MLC based classified image of LISS IV; (e) MLC based classified image of Landsat 8-OLI; (f) MLC based classified image of AWiFS

Table 4 also indicates that there is a larger difference in area calculations of agricultural land and sparse vegetation for Landsat 8-OLI and AWiFS images than that of LISS IV image. One explanation might be the misclassification between agricultural land and sparse vegetation for multi resolution satellite images. Furthermore, the LISS IV image with high spatial resolution overcomes the influence of boundary pixels and reduces the mixed pixel problems in LULC classification. It is very helpful in achieving higher OA than that of coarser spatial resolution images. The Landsat 8-OLI and AWiFS

images are not found appropriate for clearly selecting the training samples, as compared to the LISS IV image. Therefore, it is observed that LISS IV image performed significantly better in comparison to Landsat 8-OLI and AWiFS images.

Conclusions

The present study evaluates the performance of MLC for LULC classification using multi-resolution remote sensing images. In addition, the effects of spatial resolution on LULC classification accuracy are examined. It is observed that with the increase in spatial resolution, OA and Kc also increased. There is a significant increase in classification accuracy from 56 m to 5.8 m, with the moderate increase for the intermediate spatial resolution of 30 m. This study illustrates the potential of finer spatial resolution image to improve the thematic accuracy of LULC classification significantly, particularly for spectrally complex classes. The finer spatial resolution image also reduces the mixed-pixel problem to a great extent and it is found to provide more detailed information on LULC structures. Therefore, it is concluded that spatial resolution plays a vital role and influences the classification accuracy and details.

References

Borak, J.S., Strahler, A.H. (1999). Feature selection and land cover classification of a MODIS-Like data set for a semiarid environment, International Journal of Remote Sensing, 20, 5, pp. 919–938.

Chen, D., Stow, D. A., Gong, P. (2004). Examining the effect of spatial resolution and texture window size on classification accuracy: an urban environment case, International Journal of Remote Sensing, 25, pp. 1–16, 2004.

Clark, D.B., Read, J.M., Clark, M.L., Cruz, A.M., Dotti, M.F., Clark, D.A. (2004). Application of 1-m and 4-m resolution satellite data to ecological studies of tropical rain forests, Ecological Applications, 14, pp. 61-74.

Congalton, R.G., Green, K. (1999). Assessing the accuracy of remotely sensed data: principles and practices. CRC/Lewis Press, Boca Raton.

Foody, G.M., Campbell, N.A., Trodd, N.M., Wood, T.F. (1992). Derivation and applications of probabilistic measures of class membership from the maximum-likelihood classification, Photogrammetric engineering and remote sensing, 58, pp. 1335–1341.

Frank, T.D., Tweddale, S.A. (2006). The effect of spatial resolution on measurement of vegetation cover in three Mojave Desert shrub communities. Journal of arid environments, 67, pp. 88-99.

Jensen, J. (2005). Introductory digital image processing: A remote sensing perspective (3rd edition). Upper Saddle River, NJ: Prentice Hall.

Kumar, P., Gupta, D.K., Mishra, V.N., Prasad, R. (2015). Comparison of support vector machine, artificial neural network and spectral angle mapper algorithms for crop classification using LISS IV data, International Journal of Remote Sensing, 36, 6, pp. 1604–1617.

Kumar, P., Prasad, R., Choudhary, A., Mishra, V.N., Gupta, D.K., Srivastava, P.K. (2016). A statistical significance of differences in classification accuracy of crop types using different classification algorithms, Geocarto International, pp. 1-19. DOI: 10.1080/10106049.2015.1132483.

Lambin, E.F., Turner, B.L., Geist, H.J., Agbola, S.B., Angelsen, A., Bruce, J.W., Coomes, O.T., Dirzo, R., Fischer, G., Folke, C. et al. (2001). The causes of land-use and land-cover change: moving beyond the myths, Global Environmental Change, 11, 4, pp. 261–269.

Lu, D., Weng, Q. (2007). A survey of image classification methods and techniques for improving classification performance, International Journal of Remote Sensing, 28, 5, pp. 823-870.

Markham, B.L., Townshend, J.R.G. (1981). Land cover classification accuracy as a function of sensor spatial resolution, XV International Symposium on Remote Sensing of Environment, Ann Arbor.

Mishra, V.N., Rai, P.K. (2016). A remote sensing aided multi-layer perceptron-Markov chain analysis for land use and land cover change prediction in Patna district (Bihar), India, Arabian Journal of Geosciences, 9, 4, DOI: 10.1007/s12517-015-2138-3.

Mishra, V.N., Rai, P.K., Mohan, K. (2014a). Prediction of land use changes based on land change modeler (LCM) using remote sensing: a case study of Muzaffarpur (Bihar), India. Journal of the Geographical Institute Jovan Cvijic, 64, pp. 111–127.

Mishra, V.N., Kumar, P., Gupta, D.K., Prasad, R. (2014b). Classification of various land features using RISAT-1 dual polarimetric data, The International Archives of the Photogrammetry, Remote Sensing and Spatial Information Sciences, Volume XL-8: 833-837.

Moody, A., Woodcock, C.E. (1994). Scale-dependent errors in the estimation of land-cover proportions: Implications for global land-cover datasets, Photogrammetric engineering and remote sensing, 60, 5, pp. 585-596.

Richards, J. A., Jia, X. (2003). Remote sensing digital image analysis (4th edition). Heidelberg, Germany: Springer.

Salberg, B., Jenssen, R. (2012). Land-cover classification of partly missing data using support vector machines. International Journal of Remote Sensing, 33, pp. 4471-4481.

Singh, R. P., Sridhar, V. N., Dadhwal, V. K., Navalgund, R. R., Singh, K. P. (2002). Comparative evaluation of Indian remote sensing multi-spectral sensors data for crop classification. Geocarto International, 17, 2, pp. 7-12.

Swain P.H., Davis, S.M. (1978). Remote Sensing: the Quantitative Approach. New York: McGraw-Hill.

Woodcock, C.E., Strahler, A.H. (1987). The factor of scale in remote sensing. Remote sensing of Environment, 21, 3, pp. 311-332.